

## Interference Effects in Multiple Gaseous Diffusion Flames

S.K.A. Somaraj, K.S. Padiyar and R. Natarajan

*Department of Mechanical Engineering  
Indian Institute of Technology, Madras-600 036*

### ABSTRACT

Interference effects in multiple diffusion flames have been investigated. The study involved the experimental determination of flame heights of LPG diffusion flames issuing through orifices of two different diameters, viz., 1.3 and 1.7 mm, arranged in two different configurations, as a function of nozzle velocity and spacing between individual jets. The flame heights were measured from direct photographs. The interference effects arise principally as a result of oxygen starvation at close separation and lead to increased flame sizes. These effects are more pronounced in the five-burner arrangement and for the smaller orifice. They decrease with both spacing and nozzle velocity.

### NOMENCLATURE

- $a_0$  — mols air/mols fuel in nozzle fluid
- $a_r$  — mols air/mol fuel for complete combustion
- $A$  — steam or air consumption in atomiser,  $\text{nm}^3/\text{kg}$  of oil
- $A'$  — constant
- $B'$  — constant
- $C_m$  — concentration of nozzle fluid by volume on axis of jet
- $C'_f$  — value of  $C_m$  at the flame tip by volume
- $C'_T$  — stoichiometric concentration by volume
- $C_m$  — concentration of nozzle fluid by weight on axis of jet
- $C_f$  —  $C_m$  at the flame tip by weight

- $C_T$  — stoichiometric concentration by weight  
 $d_0$  — true nozzle diameter  
 $d_0'$  — equivalent nozzle diameter  
 $d$  — diameter of jet at a distance  $x$  downstream from nozzle  
 $D$  — diffusivity, co-efficient at flame temperature  
 $D_0$  — diffusivity co-efficient at room temperature  
 $F$  — calorific value of gas  
 $g$  — acceleration due to gravity  
 $G_0$  — jet momentum flux at burner exit  
 $G_{obs}$  — observed thrust  
 $K_f$  — calorific value factor  
 $L_f$  — flame length  
 $LPG$  — liquefied petroleum gas  
 $L_{ch}$  — chemical flame height  
 $L_{SIF}$  — length of a single isolated flame  
 $m_0$  — jet mass flux at burner exit, kg/s  
 $M_0$  — molecular weight of the combustion products at burner exit  
 $M$  — molecular weight of the ambient air  
 $m_{oil}$  — mass flow rate of oil  
 $m_s$  — mass flow rate of steam  
 $m_{aT}$  — mass flow rate of theoretical air  
 $Q$  — volumetric flow rate of fuel  
 $s$  — break point length  
 $S$  — volume of air/volume of fuel gas for complete combustion  
 $t$  — time  
 $T_E$  — nozzle exit temperature ( $^{\circ}K$ )  
 $T_f$  — flame temperature ( $^{\circ}K$ )  
 $T$  — ambient air temperature ( $^{\circ}K$ )  
 $U_0$  — nozzle exit velocity  
 $W_s$  — molecular weight of the surrounding fluid  
 $W_0$  — molecular weight of the nozzle fluid  
 $W_i$  — mass fraction of source stream material in a stoichiometric mixture with air, kg/kg  
 $X_0$  — mol fraction of fuel counted unreacted at burner exit  
 $X$  — mol fraction of fuel at the flame axis in a stoichiometric mixture  
 $a$  — ratio of the mols of reactants to number of mols of combustion products

- ratio of molecular weight of combustion products at any position to molecular weight of unburned mixture
- $\rho_0$  — density of jet fluid
- $\rho_\infty$  — density of ambient air
- $\rho_f$  — density of final mixture
- $\mu_\infty$  — viscosity of ambient air
- $\theta_f$  — generalised time at flame tip

## 1. INTRODUCTION

In some practical gas burners, the fuel gas stream is subdivided into a number of single jets, so that the resulting flame is shortened considerably. Depending on the distance between the orifices, individual or merged flames would be produced. In solid-propellant rocket ramjet engines, fuel-rich propellant gases are discharged from the primary chamber to the secondary combustor through sets of orifices of prescribed geometry. The subsequent combustion occurs on mixing with ram air drawn through intakes. These combustion phenomena may be modelled either in terms of a well-stirred reactor or as individual diffusion flames subjected to interference effects and confinement.

When jet flames are arranged in groups, the interference between the individual jet flames results in increased length of the flames in the centre of the group, and also adversely affects the stability of these flames<sup>1</sup>. If the pitch to diameter ratio is reduced below a critical value for a group of three flames in a row, Allen<sup>2</sup> has shown that the central flame will be extinguished. The principal reason is that the neighbouring flames restrict each other's access to air and suffer oxidizer-starvation. At large separation distances, however, there will be no noticeable interaction between the individual jets in the groups.

Tables 1 and 2 in Appendix summarise the principal results of earlier investigations on the length of laminar and turbulent diffusion flames.

## 2. CRITERIA FOR FLAME LENGTH

There are several different criteria adopted by different workers for characterizing the length of diffusion flames<sup>3</sup>.

- (i) The thermal measure of flame length or thermal flame height,  $L_{th}$  is defined as the distance along the flame axis from the burner exit where the maximum of mean flame temperature lies on the flame axis.
- (ii) The chemical measure of flame length,  $L_{ch}$  is defined with reference to the position of minimum carbon monoxide (CO) concentration on the flame axis. The flame tip is taken to be the point on the flame axis where the CO concentration is less than 0.1 per cent. It is also characterised by the distance along the flame axis,

where the mass fraction of fuel on the flame axis is equal to the fuel mass fraction in a stoichiometric mixture with ambient air.

- (iii) The visible flame length,  $L_f$  is determined either visually by a trained observer viewing the flame against a dark background or from direct photographs of appropriate duration. The flame tip is located at the furthest down stream point at which elements of flame front appear with appreciable frequency.
- (iv) The flame height is also determined using soot concentration measurements along the axis of the flame<sup>4</sup>. If hydrocarbons are the only species present in the flame, the axial soot maximum may be expected to represent the end of the diffusion flame. With methane/air flames, sufficient quantities of  $H_2$  and CO were also present, and a correction factor was applied. However, this method is not very satisfactory in view of the widely differing soot-forming tendencies of fuels and under different operating conditions.

According to the Burke and Schumann theory postulated for laminar flames, all the above measures must be identical. However, in turbulent diffusion flames, and even in the usually non-steady laminar diffusion flames, the visible flame length may be greater than  $L_{ch}$  or  $L_{th}$  due to the effects of billowing and flickering. These erratic motions produce a statistical thickening of the flame front about the surface where the fuel fraction is equal to the stoichiometric value, and a lengthening of the flame beyond  $L_{ch}$ . The visible flame tip, as judged by the eye, may be different for different observers, but within limits<sup>5</sup> of  $\pm 5$  to  $\pm 15$  per cent.

At certain nozzle velocities, it has been found that either the normal on-port flame or an off-port or lifted flame can be produced. Hawthorne *et al.*<sup>6</sup> have measured the visible flame length of lifted flames from the lift-off plane to the flame tip. According to Becker and Liang<sup>5</sup>, visible flame length should be measured from the effective start of the gas jet to the visible flame tip even when the combustion zone commences at some distance downstream. Lift-off appears to lengthen some flames slightly but measurably<sup>5</sup>. In the present study, lifted flames were avoided by employing stabiliser rings, and the flame height is measured from the burner exit to the flame tip.

### 3. PRESENT WORK

The effect of interference on the flame height of LPG flames issuing through orifices of two different diameters, viz., 1.3 and 1.7 mm, arranged in two different configurations has been studied here. The average composition of LPG used is  $C_2H_6 = 0.148$  per cent,  $C_3H_8 = 6.734$  per cent, iso- $C_4H_{10} = 16.536$  per cent and normal- $C_4H_{10} = 76.582$  per cent.

The experimental set-up (Fig. 1) consisted of a conical diffuser (semi-cone angle :  $12^\circ$ ), a settling chamber and a nozzle. A rotameter, calibrated for the fuel gas, measured the fuel flow. The nozzle provides a uniform velocity profile for the fuel gas, and burner plates with different configurations of burner orifices are mounted at the nozzle exit. At low exit velocities, the flames were attached to the burner plate:

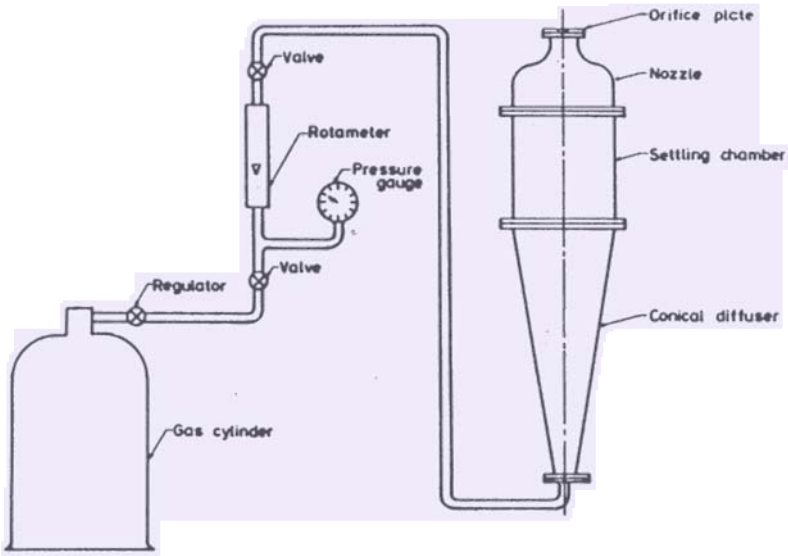


Figure 1. Experimental set-up for studies on multiple diffusion flames.

However, at higher velocities the flames tended to lift-off the burner ports. In order to stabilise the flames on the burner plate, a stabiliser ring was used; the dimensions of which depend on the diameter of the jet and the burner geometry under investigation.

The flame height was measured by taking direct photographs of the flames with an exposure time of 2 sec. A scale is photographed along with the flame for better accuracy. These measurements were verified by those obtained by visual observation, which are affected by subjective considerations. The photographs yield time-averaged flame heights.

The experiments were conducted for each orifice size, and for each group configuration, over a range of separation (expressed in terms of pitch circle diameter varied from 5 to 27 mm), and a range of nozzle velocities. The flame heights are compared with those of a single isolated flame at the same nozzle velocity.

#### 4. RESULTS AND DISCUSSION

Figure 2 shows the effect of spacing on the variation of normalised flame length with nozzle velocity, for the 1.3 mm jet diameter flames, for the double-jet configuration. For a particular spacing,  $L_f/d$  increases as the nozzle velocity is increased, and attains a constant value when the flames become fully turbulent. For a particular nozzle velocity,  $L_f/d$  decreases as the spacing increases. The value of  $L_f/L_{SIF}$  increases initially as the nozzle velocity is increased, and then decreases. It decreases as the spacing is increased, at a certain nozzle velocity. As mentioned earlier,  $L_f$  and  $L_{SIF}$  are compared at the same values of nozzle velocity.

Figure 3 shows the same results for the five-burner arrangement. While  $L_f/d$  shows the same sort of variation with the velocity as in the earlier case, the values of

$L_f/d$  are much higher at each velocity, indicating higher levels of interference in this case. Unlike in the earlier case,  $L_f/L_{SIF}$  decreases rapidly with increase in velocity up to about 15 m/s and then remains essentially constant.

Figure 4 shows the effect of nozzle velocity on the variation of normalised flame length with spacing for the two-burner arrangement. As noted earlier, both  $L_f/d$  and  $L_f/L_{SIF}$  decrease as the spacing is increased, as a result of decreasing levels of interference. The top graph shows  $L_f/L_{SIF}$  for the 1.7 mm jets also.

Figure 5 shows the above results for the five-burner arrangement. As noted earlier,  $L_f/d$  shows trends similar to the two-burner arrangement, but the values of

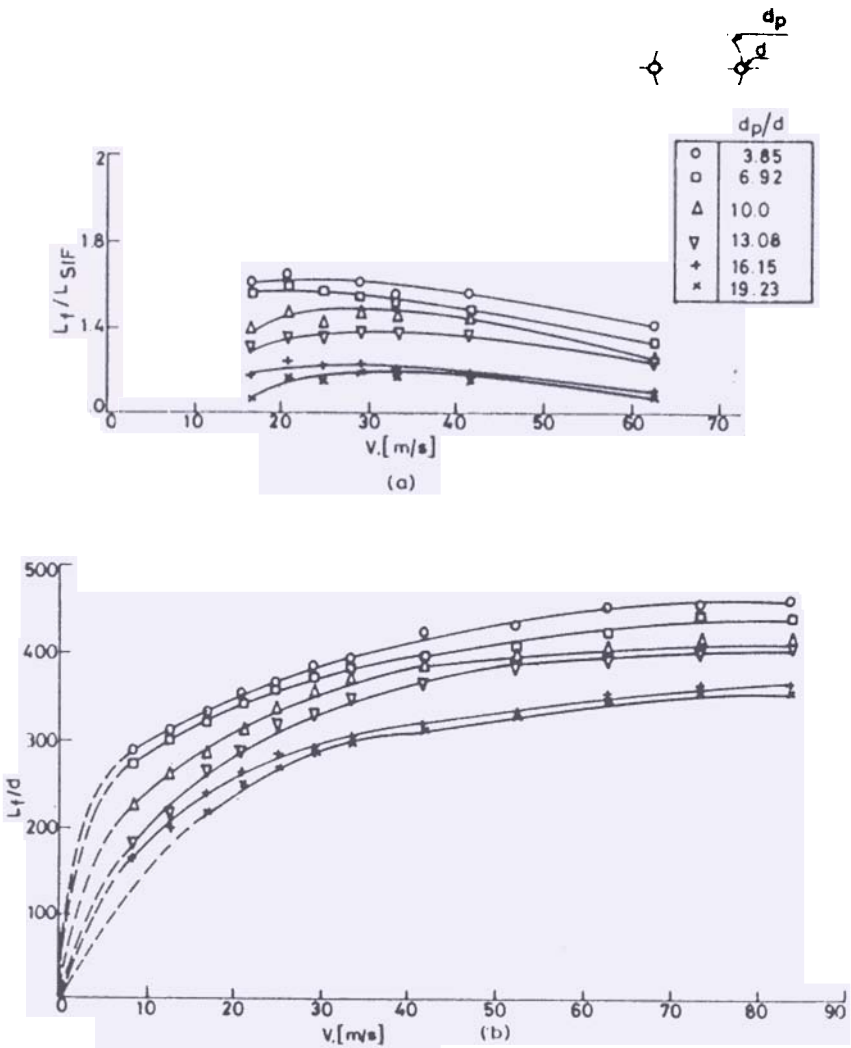


Figure 2. Effects of the nozzle velocity and the jet spacing on the flame length (two-burner configuration (diameter of orifice = 1.3 mm)).

$L_f/d$  are higher.  $L_f/L_{SIF}$  values are also much higher than for the earlier case. These values are larger for the 1.3 mm jets than for the 1.7 mm jets at the same velocity and spacing.

Figures 6 and 7 show the photographs for the 1.3 mm jet flames, for the two and five-burner arrangements, respectively. In Fig. 6, the top series shows the variation of flame size and shape with spacing at a nozzle velocity of 16.74 m/s, corresponding to  $Re = 6544$ , while the bottom series corresponds to a nozzle velocity of 20.93 m/s,

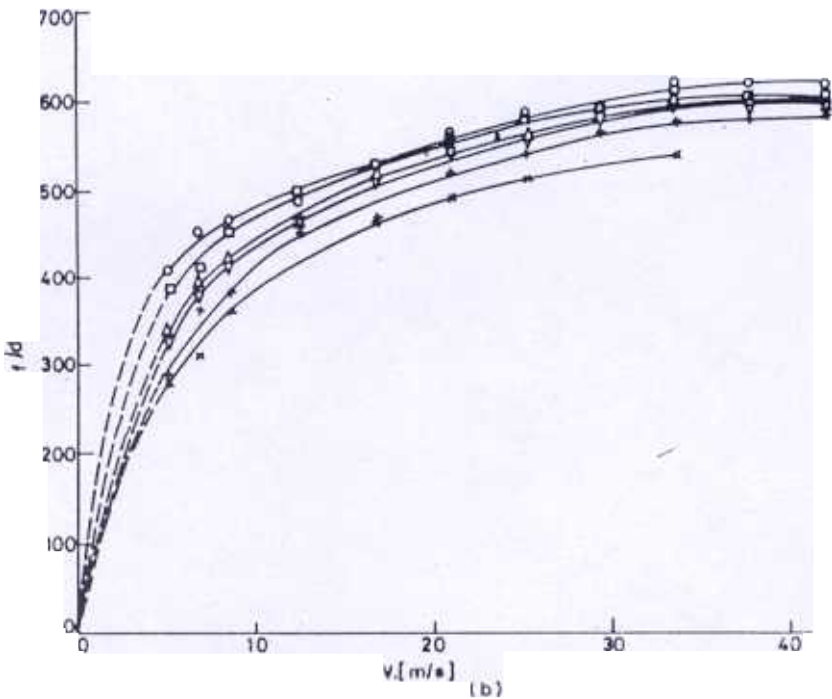
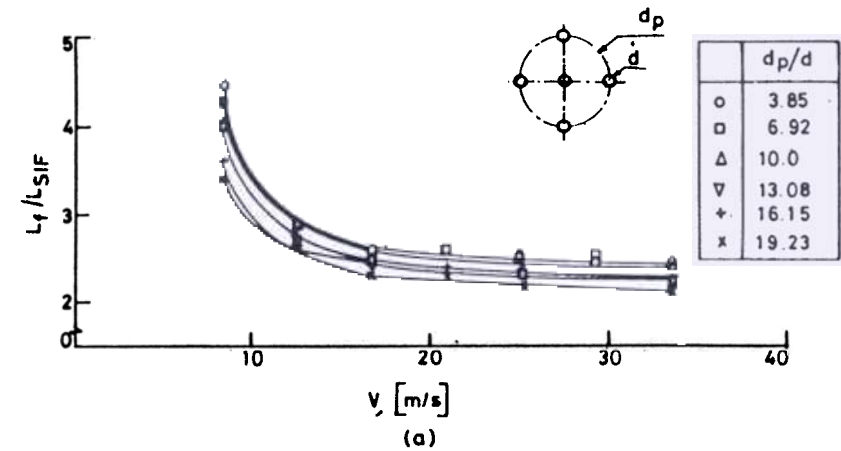


Figure 3. Effects of the nozzle velocity and the jet spacing on the flame length five-burner configuration (diameter of orifice = 1.3 mm).

equivalent to  $Re = 8182$ . For comparison, a single isolated flame, at the same nozzle velocity is also shown. The increase in length and merging of the flames with decreasing spacing can be observed. For the five-burner arrangement (Fig. 7), the flames are much larger, and even at a spacing of 25 mm, the interference effects are quite considerable.

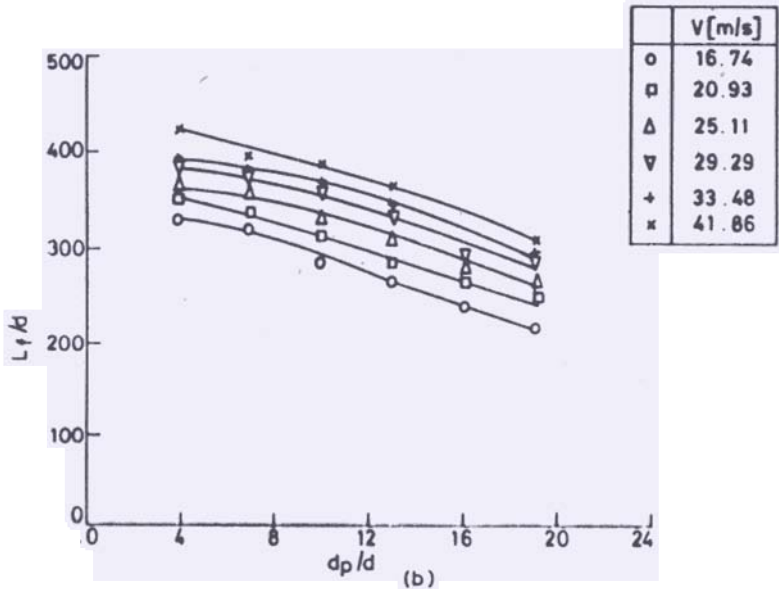
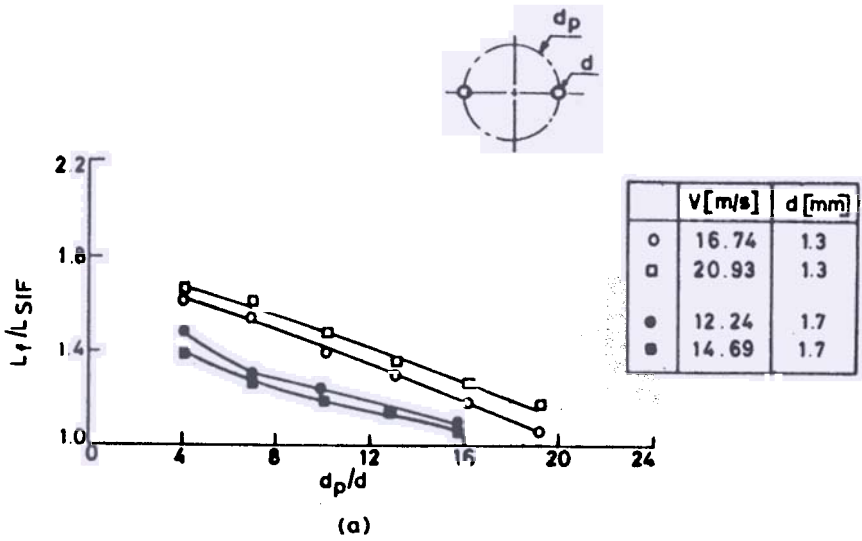


Figure 4. Effects of the normalised spacing and the nozzle velocity on the flame length ; two-burner configuration.



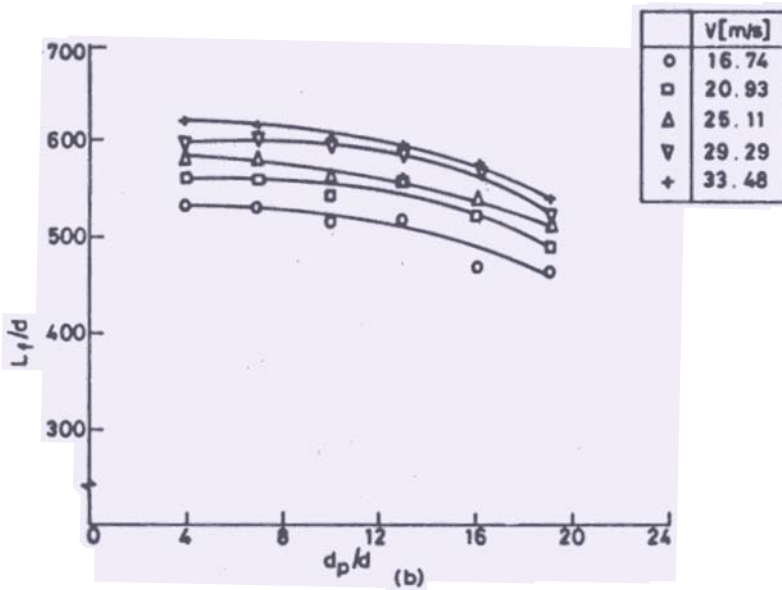
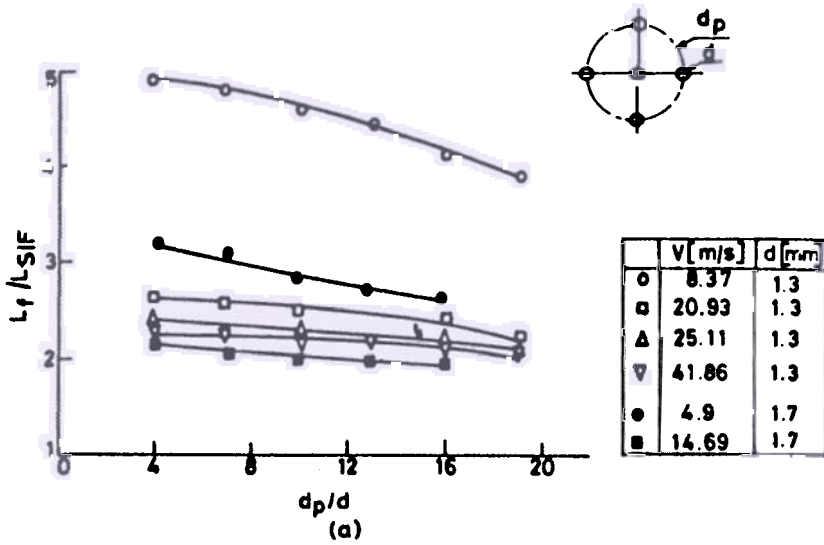


Figure 5. Effects of the normalised spacing and the nozzle velocity on the flame length : five-burner configuration.

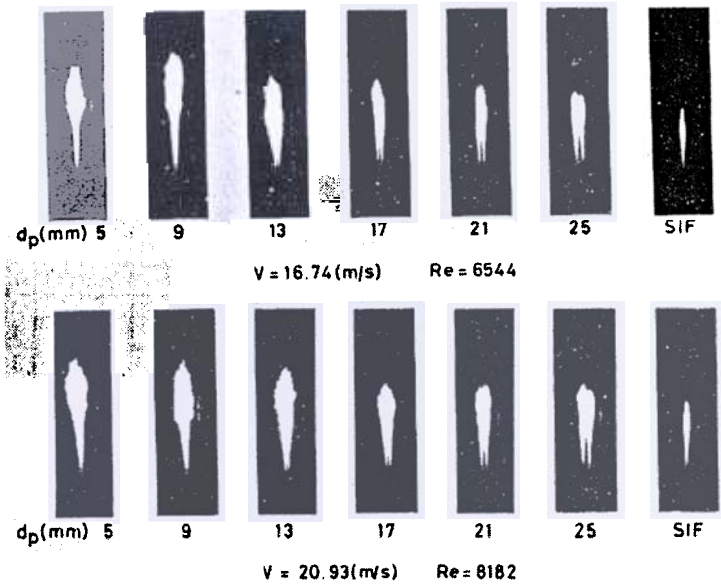


Figure 6. Indane gas flames for two-burner arrangement (diameter of jet 1.3 mm).

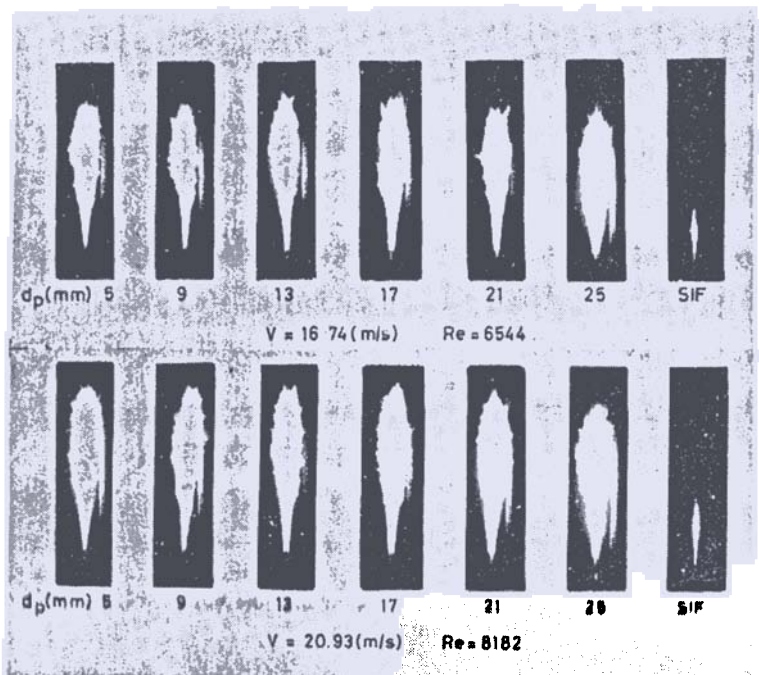


Figure 7. Indane gas flames for five-burner arrangement (diameter of jet 1.3 mm).

## 5. CONCLUDING REMARKS

The interference effects in multiple diffusion flames have been investigated here as a function of individual jet size, nozzle velocity and spacing of individual jets, for two different burner arrangements. The interference effects are basically a result of the restriction of access to the available air. The interference effects are more in the five-burner arrangement than in the two-burner arrangement. They decrease with spacing, decrease with nozzle velocity, and are higher for the smaller orifice investigated.

## REFERENCES

1. Beer, J.M. & Chigier, N.A., *Combustion Aerodynamics*, (John Wiley, New York), 1972.
2. Allen, R.A., PhD. Thesis, The University of Sheffield, UK, 1970; cited in ref. 1.
3. Ebrahim, S.M.A. & El-Mahallawy, F.M., *Comb. and Flame*, **60** (1985), 141-155.
4. Roper, F.G., Smith, C. & Cunningham, A.C., *Comb. and Flame*, **29** (1977), 227-234.
5. Becker, H.A. & Liang, D., *Comb. and Flame*, **32** (1978), 115-137.
6. Hawthorne, W.R., Weddell, D.S. & Hottel, H.C., Mixing and combustion in turbulent gas jets, *In Third Symposium on Combustion, Flame and Explosion Phenomena*, 1949, pp. 266-288.
7. Jost, W., *Explosions and Verbrennungs in Gasen*, (Springer, Berlin), 1939.
8. Hottel, H.C. & Hawthorne, W.R., Diffusion in laminar flame jets, *In Third Symposium on Combustion, Flame and Explosion Phenomena*, 1949, pp. 254-266.
9. Wohl, K., Gaszley, C. & Kapp, N., Diffusion flames, *In Third Symposium on Combustion, Flame and Explosion Phenomena*, 1949, pp. 288-300.
10. Roper, F.G., *Comb. and Flame*, **29** (1977), 219-226.
11. Rambert, E.W. & Haslam, R.T., *Ind. Eng. Chem.*, **20** (1925), 1236.
12. Kunugi, M., Osumi, K. & Yoshida, K., Studies on the Vertical Diffusion Flame, (Faculty of Engg., Kyoto University, Kyoto).
13. Leys, J.A., *BISRA P/N*, (1953), 202.
14. Sunavala, P.D., *Chemical Age of India*, (1960), 217-227.
15. Günther, R., *Gaswärme*, **15** (1966), 376.
16. Becker, H.A. & Yemazaki, *Comb. and Flame*, **33** (1978), 123-149.
17. Thing, M.W. & Newby, M.P., Combustion length of enclosed turbulent jet flames, *In Fourth Symposium (Int.) on Combustion*, 1952; pp. 789-796.
18. Ievechenko, P.V. & Kitayev, B.I., *Stahl*, **3** (1952).

Table 1(a). Correlations for length of laminar flames – theoretical studies

Sl. No.	Source	Expression	Assumptions	Applicability	Remarks
	Ref. 7	$L_f = \frac{Q}{U_0}$	$D$ is constant $x^2 = Dt$ $U_0$ is constant along the axis	Flame length < 15 cm	The expression does not consider the air requirement for combustion. Constancy of $U_0$ assumption along the axis is unsatisfactory for flames > 15 cm.
2.	Ref. 8	$L_f = \frac{Q\theta_f}{\pi D}$	$D$ is constant $U_0$ is constant along the flame axis $1/\theta_f = -4 \ln \left( \frac{a_f - a_0}{1 + a_f} \right)$	Flame length < 15 cm Primary fuel jet of higher velocity issuing into an infinite atmosphere of air.	Constancy of $U_0$ assumption along the jet axis is unsatisfactory for flames > 15 cm. Allowance is made for different gases in the factor $\theta_f$ .
	Ref. 9	$L_f = \sqrt{\frac{2\pi K C_f'}{Q \left(1 - \frac{C_f'}{2}\right)} + \frac{2\pi D_0 C_f'}{Q \left(1 - \frac{C_f'}{2}\right)}}$	$D = D_0 + KL_f$ $K$ is a constant	For all gases	$D_0$ and $K$ vary with gas composition.
4.	Ref. 10	$\frac{L_f}{Q} = \left\{ 4D_0 \ln 1 + \frac{1}{S} \right\}^{-1} \times \left( \frac{T_w}{T_f} \right)^{0.67}$	Temperature and diffusivity are constant throughout the flame. Axial diffusion is neglected. Schmidt number (Sc) and Lewis number (Le) are unity.	For circular port burner	The expression is obtained by modifying the Burke-Schumann theory, so as to satisfy continuity when the fuel gas velocity differs from the value at the burner port.

Table 1(b). Correlations for length of laminar flames – experimental studies

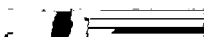
Sl. No.	Source	Expression	Assumptions	Applicability	Remarks
	Ref. 11	$L_f = f_1(a_0) \log_{10} U_0 + f_2(a_0) \log_{10} d_0 + f_3(a_0)$		Flame length > 15 cm	$f_1(a_0)$ , $f_2(a_0)$ and $f_3(a_0)$ are three different functions of $a_0$ .
	Ref. 8		$D$ is constant $A'$ and $B'$ are constants, independent of flow and diameter	Flame length > 15 cm	$A'$ and $B'$ are different for different gases.
3.	Ref. 9	$1. L_f = \frac{1}{\frac{0.206}{\sqrt{Q}} + \frac{0.354}{Q}}$ $2. L_f = 4.3 d_0 U_0^{0.5}$	$D = D_0 + KL_f$ $K$ is a constant	For city gas	$L_f$ and $d_0$ in cm; $U_0$ in cm/s.
4.	Ref. 12	$L_f = \frac{(U_0 d_0) q_0^{0.5}}{4.08 + 0.0085 (U_0 d_0)}$	$D = D_0 + KL_f$ $K$ is a constant.	For coal gas and water gas	$L_f$ and $d_0$ in cm; $U_0$ in cm/s.

Table 2(a). Correlations for length of turbulent flames – theoretical studies

Sl. No	Source	Expression	Assumptions	Applicability	Remarks
Ref. 6		$\frac{L_f}{d_0} = \frac{5.3}{C_T'} \sqrt{\frac{T_f}{dT_E}} \sqrt{\left\{ C_T' + (1 - C_T') \frac{W_f}{W_0} \right\}}$	Negligible buoyancy and constancy of momentum transport across all sections of jet profile	Applicable only up to the point of stoichiometric composition	This equation is for the forced convection limit. Flame length is measured from the lift-off plane to the flame tip.
Ref. 9		$\frac{L_f}{d_0} = \frac{1}{0.0408 C_T' C_T'}$		For all gases	
3. Ref. 13		$L_f = \frac{6.5 (m_{oil} + m_{air})}{\sqrt{\rho g C_{obs}}}$			
4 Ref. 14				For gaseous flames	
5. Ref. 15		$\frac{L_f}{d_0} = 6(R + 1)(\rho_d/\rho_f)^{1/2}$		For gaseous flames	The expression has been found to be accurate within 10%.
6 Ref. 16		$\frac{L_f}{d_{eq}} = \frac{11\beta}{W_1}$	Buoyancy is negligible $\xi_L < 1$ and $Re_L > 8000$		$d_{eq} = (4m^2/\pi\rho_w a_0)^{1/2}$ $\beta = (M_\infty T_1/M_1 T)^{1/2}$ $\xi_L = (\pi g \rho_w / 4G)^{1/3} L_f$ $Re_L = \pi m_0 \beta / \mu_\infty W_1 L_f$
Ref. 3		$\frac{L_{sh}}{d_0} = 5.3 \frac{X_0}{X_s} \left[ \left\{ \frac{X_s}{X_0} + \frac{M}{M_0} \left( 1 + \frac{X_s}{X_0} \right) \right\} \frac{T_f}{T_E} \right]^{1/2}$	Buoyancy is negligible	For gaseous flames with co-flowing fuel and air	The flame tip is considered as the point on the flame axis with maximum CO <sub>2</sub> concentration.

Table 2(b). Correlations for length of turbulent flames – experimental studies

Source	Expression	Assumptions	Applicability	Remarks
	$\frac{L_f}{d_0} = \frac{0.0075 + 3.8}{U_0}$		For city gas	The basis for this expression is the concept of eddy diffusivity.
	$\frac{L_f}{d_0} = \frac{0.0132 + \frac{3.23}{U_0}}$		For a mixture of 50% city gas in air	
	$L_f = \frac{5.3d_0'}{C_T} \pm 10\%$		For oil and gaseous flames	For gaseous flames $d_0' = d_0 \sqrt{\rho_0 \rho_f}$ $1/C_T = (m_{oil} + m_{sT})/m_{oil}$ For oil flames, $d_0' = 2(m_{oil} + m_s)/\sqrt{\rho_f g G_{obs}}$
				$\frac{1}{C_T} = \frac{m_{oil} + m_s + m_{sT}}{(m_{oil} + m_s)}$
Ref. 18	$\frac{L_f}{d_0} = (0.0026F + 1.12)$	For gas, $k_f = 0.016\sqrt{F}$ ; For oil,	For gaseous flames < 15 cm, with burner nozzles less than 20 mm in diameter,  For oil flames < 15 cm, with burner nozzles less than 20 mm in diameter.	F : calorific value of gas in kcal/m <sup>3</sup>
	$\frac{L_f}{d_0} = 0.2(0.0026F + 1.12),$	$k_f = 0.016 \sqrt{\frac{10000}{A + 0.5}}$		
	$L_f = 14k_f d_0^{0.83} U_0^{0.34}$		For oil and gaseous flames > 15 cm with burner nozzles greater than 20 mm diameter.	